Author version

Published as:

Sandoval, S. A., Lu, P., Hwang, J. T., Rea, J. R., & Sostaric, R. R. (2022). Multiple optima in abort ascent during lunar powered descent. In AIAA SCITECH 2022 Forum (Paper No. AIAA 2022-0949). https://doi.org/10.2514/6.2022-0949

BibTeX for this reference:

https://lsdolab.github.io/lsdo-publications/publication/sandoval2022multiple/

```
@inproceedings{sandoval2022multiple,
  author = {Sergio A. Sandoval and Ping Lu and John T. Hwang and Jeremy R. Rea and Ronald
    R. Sostaric},
  title = {Multiple Optima in Abort Ascent during Lunar Powered Descent},
  booktitle = {AIAA SCITECH 2022 Forum},
  year = {2022},
  doi = {10.2514/6.2022-0949},
  url = {https://doi.org/10.2514/6.2022-0949}
}
```

Multiple Optima in Abort Ascent during Lunar Powered Descent

Sergio A. Sandoval* and Ping Lu†
San Diego State University, San Diego, CA 92182

John T. Hwang‡
University of California, San Diego, CA 92093

Jeremy R. Rea§ and Ronald R. Sostaric¶
NASA Johnson Space Center, Houston, TX 77058

In the course of a human mission to land on the Moon, adverse circumstances can turn success into chaos. Minimal effort has been spent to improve previous abort guidance techniques since the Apollo era. An abort guidance approach based on the indirect method of optimal control has shown that a solution to this complex problem can be found online for most of the descent trajectory. A deeper examination of the abort guidance solution identified an undiscovered phenomenon that caused some trajectories to converge to lower altitudes than their neighboring solutions. The discovery of multiple solutions in the abort guidance problem gives an explanation to this phenomenon and is the focus of this work. The complete formulation of the problem and method of solution are shown, as well as the implications for future lunar landing missions. The findings are pertinent to any abort guidance regardless of its implementation and it becomes an important topic for discussion regarding mission planning and astronaut training. Validation and verification of the algorithm and its results has been achieved with an implementation of the problem with the direct method of optimal control.

I. Introduction

Sixty years have passed since President John F. Kennedy committed this nation to reach the Moon by the end of the decade. Amid a period of great uncertainty and tension with Russia, the space program in the United States set its sights to the Moon and started to work in one of the greatest endeavors of humankind [1]. Testing and development between 1961 and 1969 led to the historical landing on the Moon on July 20th, 1969. As part of the development, flight simulations with astronauts were performed routinely to practice maneuvers and improve spacecraft control and handling [2–5]. Computational capabilities of the era were much less competent than any computer of our time [6]. Despite the absence of computer power, the demands of the space program were by no means easily accomplished and engineers at that time had to solve these problems with the tools available. Ever since Apollo, there has been a period of great technological development that has sparked interest in applying the most recent techniques in optimization to solve some of the same problems in a more efficient way. Thanks to all these technological advances, difficult problems involving more rigorous computations can be solved. These changes have taken place in many areas of research, particularly in the areas of optimal control and numerical optimization.

During the planning of Apollo, abort capability was a subject of much attention [7, 8]. The importance of crew safety was evident by the amount of redundancy and studies of a multitude of possible emergency scenarios. Each one of these scenarios was analyzed and appropriate abort techniques were put into place at any given time during the mission. Part of this process was the constant training of astronauts in simulators to practice as many contingencies as possible. By spending a great amount of time training in preparation for such events, a high level of confidence could be attained to guarantee that every single member of the crew would return safely to Earth. In contrast, there has been minimal attention on the subject regarding abort guidance during powered descent for Artemis.

*Graduate Research Assistant, Department of Aerospace Engineering, ssandoval4327@sdsu.edu. Student Member AIAA.
†Professor and Chair, Department of Aerospace Engineering, plu@sdsu.edu. Fellow AIAA.
‡Assistant Professor, Department of Mechanical and Aerospace Engineering. Member AIAA.
§Aerospace Engineer, Flight Mechanics and Trajectory Design Branch, 2001 NASA Parkway - EG5. AIAA Member
¶SPLICE Project Manager, Flight Mechanics and Trajectory Design Branch, 2001 NASA Parkway - EG5. AIAA Senior Member.

Recently, an optimal control guidance approach was shown to have solved the complex problem of abort during powered descent landing on the Moon [9]. The technique is based on the indirect method of optimal control and utilizes an advanced propellant-optimal guidance approach named the Universal Powered Guidance (UPG) [10]. A version of ascent guidance with this approach is called UPG+A. UPG+A was used to insert a spacecraft from an initial descent trajectory into a safe pericynthion orbit around the Moon. A free-attachment-point was implemented to allow the algorithm to find out the best insertion point. The task was accomplished by the implementation of a two-phase maneuver: a pull-up phase and a fuel-optimal ascent phase. On the first phase, it is the responsibility of the pull-up maneuver to turn the velocity vector of the vehicle by changing the flight path angle from negative to positive. This is necessary to point the vehicle in a more favorable direction to start ascent. Then, the optimal ascent guidance takes over the final state of the pull-up maneuver and controls the spacecraft until the preplanned safe orbit is reached with minimum propellant consumption. Reference [9] shows how this operation was performed flawlessly for a mission to land the Apollo lunar lander at the South Pole of the Moon. The concept of operation for the abort guidance developed in Reference [9] is shown in Fig. 1.

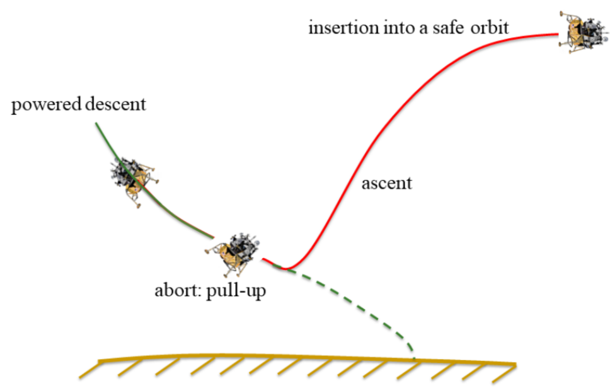

Fig. 1 Abort Guidance Concept of Operations [9]

The flight time of the nominal powered descent trajectory from the start of the powered descent initiation (PDI) until touchdown is of 610 seconds, and a solution was found for abort scenarios between 0 and 600 seconds. For most of the trajectory, UPG+A was able to obtain a solution and it only failed to converge in cases that were very late in the descent. After 600 seconds, it is safe to assume that the spacecraft is so far down that it would be implausible to rotate the velocity vector fast enough to avoid a collision to the ground. Perhaps, at that point it would be safer to continue the powered descent guidance all the way to the ground and try to reduce the velocity as much as possible. Moreover, Monte Carlo simulations were performed to test the algorithm under more stringent conditions. Dispersions on the initial conditions of the powered descent trajectories were enforced at 3000 uniformly distributed times during the descent flight. The algorithm performed this task without a problem even when amplifying the dispersions by up to 5 orders of magnitude.

Despite the amazing results obtained, an unforeseen circumstance lingered among the solution without a clear explanation. Almost all the trajectories obtained followed an altitude pattern that ended at an orbit radius similar to its neighboring solutions. Amid the solutions, some of the trajectories separated from the final altitude pattern and successfully converged to a lower altitude. Figure 2 shows the resulting trajectories of 3000 abort cases along the powered descent trajectory in a mission to land a spacecraft on the Moon.

The figure demonstrates that some of the abort cases appear to be inconsistent with the rest. At first sight, it appears that these cases failed to meet the terminal conditions successfully, but a closer look shows that each of the abort trajectories successfully delivers the vehicle to the specified final orbit. Given that the safety of the crew is the most important part of the mission, gaining an understanding of the potential outcomes during an emergency is of vital importance. This is particularly relevant during to astronaut training since a large portion of it involves exercises to prepare for unexpected circumstances. Through careful exploration of the solution, these inconsistent cases were analyzed to find the cause of the sudden discontinuity in orbital insertion altitude. Analyzing the elements of the final orbit such as eccentricity, semi-major axis, and inclination, demonstrated that the discrepant cases were indeed inserted into the correct orbit. Furthermore, sampling some of these cases at different true anomalies and recording the propellant consumption revealed that multiple optimal solutions exist for most of the abort scenarios during powered descent. An inspection of the true anomaly across the different cases uncovered that some of these cases end up at local minimum

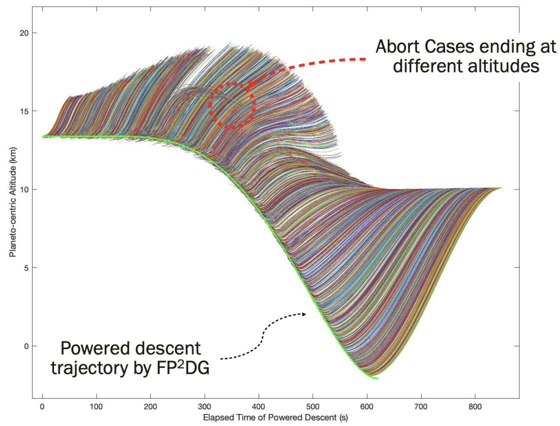

Fig. 2 Abort-ascent trajectories at different points throughout powered descent

rather than the global minimum of the ascent problem. It is the goal of this paper to demonstrate the rationale behind this phenomenon and to provide validation and verification of this discovery using the direct and indirect methods of optimal control.

II. Abort Guidance Problem

The abort guidance problem is separated in two phases: a pull-up maneuver and an optimal ascent guidance phase. The pull-up maneuver is necessary to position the vehicle in a suitable direction to start optimal ascent. This is accomplished by the rapid change of a negative descent flight path angle towards a positive flight path angle ready for ascent. The fastest way to achieve these changes is by pointing the thrust vector in a direction perpendicular to the velocity vector of the vehicle. Three different guidance laws were developed in to complete this maneuver. The complete derivation of the pull-up maneuver can be found on Reference [9]. In this paper, a general ascent guidance problem is solved. The three-dimensional equations of motion for a vehicle with rocket propulsion defined as a point-mass system in a Cartesian coordinate system are defined as follows:

$$\dot{\boldsymbol{r}} = \boldsymbol{V} \tag{1}$$

$$\dot{\boldsymbol{V}} = \boldsymbol{g}(\boldsymbol{r}) + \frac{T}{m(t)}\mathbf{1}_T \tag{2}$$

$$\dot{m} = -\frac{T}{g_0 I_{sp}} = -\frac{T}{v_{ex}} \tag{3}$$

The origin of the equations is at the center of the Moon. The equations describe the dynamics of the rocket as it moves around the Moon with $\boldsymbol{r} \in R^3$ and $\boldsymbol{V} \in R^3$ specifying the position and velocity, respectively.

In an abort scenario, the thrust magnitude T is always at full throttle, $T(t) = T_{max}$. Hence, the only control variable available is the thrust direction $\mathbf{1}_T(t)$, changing with time. For a small variation of the radius, as it is the case in the ascent problem, the following formulation for the gravitational acceleration of g can be applied [11]:

$$\boldsymbol{g}(\boldsymbol{r}) = -\frac{\mu}{r^3}\boldsymbol{r} \tag{4}$$

The performance index is selected to minimize the propellant consumption of the vehicle at full throttle:

$$J = \int_{t_0}^{t_f} -\frac{T_{max}}{v_{ex}} dt = m(t_f) - m(t_0) \tag{5}$$

Where T_{max} is the constant maximum thrust of the rocket required to escape as fast as possible during an emergency and v_{ex} is the escape velocity of the rocket on Earth. This is equivalent to minimizing the propellant consumption during ascent.

A total of 7 algebraic equations are solved simultaneously by UPG+A to solve the ascent guidance problem. These equations represent the orbital insertion conditions for the final orbit and the corresponding reduced transversality conditions [12].

$$(\boldsymbol{r}_f \times \boldsymbol{V}_f)^T (\boldsymbol{r}_f \times \boldsymbol{V}_f) - \mu a^*(1 - e^{*2}) = 0 \tag{6}$$

$$\frac{\boldsymbol{V}_f^2}{2} - \frac{\mu}{\boldsymbol{r}_f} + \frac{\mu}{2a^*} = 0 \tag{7}$$

$$\mathbf{1}_z^T (\boldsymbol{r}_f \times \boldsymbol{V}_f) - |\boldsymbol{r}_f \times \boldsymbol{V}_f| cos(i^*) = 0 \tag{8}$$

The final altitude and velocity vectors to be found by the optimization algorithm are represented by r_f and V_f, with their norms $\boldsymbol{r}_f = ||\boldsymbol{r}_f||$ and $\boldsymbol{V}_f = ||\boldsymbol{V}_f||$, respectively. The predetermined values of semi-major axis, eccentricity, and inclination for the final orbit are defined by a^*, $e^* \neq 0$, and $i^* \neq 0$. The vector 1_z is unit vector parallel to the polar axis of the Moon pointing towards the North. The orbital conditions selected correspond to a free-attachment-point case, where the final position and velocity of the spacecraft is not specified. It is the duty of the algorithm to find the best position and velocity for orbital insertion.

The 3 transversality conditions required to solve the indirect method problem are related to the 3 free orbital elements of the problem that are argument of perilune, longitude of the ascending node and true anomaly at the insertion point [12]:

$$(\boldsymbol{p}_{r_f} \times \boldsymbol{r}_f + \boldsymbol{p}_{V_f} \times \boldsymbol{V}_f)^T (\boldsymbol{r}_f \times \boldsymbol{V}_f) = 0 \tag{9}$$

$$(\boldsymbol{p}_{r_f} \times \boldsymbol{r}_f + \boldsymbol{p}_{V_f} \times \boldsymbol{V}_f)^T \mathbf{1}_z = 0 \tag{10}$$

$$\boldsymbol{p}_{r_f}^T \boldsymbol{V}_f - \frac{\mu}{r_f^3} \boldsymbol{p}_{V_f}^T \boldsymbol{r}_f = 0 \tag{11}$$

In these equations, the costate vectors for radius and velocity at the final time t_f in the optimal ascent problem are $\boldsymbol{p}_{r_f}$ and $\boldsymbol{p}_{V_f}$. A final transversality condition at t_f related to the Hamiltonian for free-time optimal control problems completes the set of 7 algebraic equations that UPG+A needs to solve [12]:

$$\boldsymbol{p}_{r_f}^T \boldsymbol{V}_f - \mu \boldsymbol{p}_{V_f}^T \boldsymbol{r}_f + T_{max} \frac{||\boldsymbol{p}_{V_f}||}{m(t_f)} - 1 = 0 \tag{12}$$

The complete set of equations to solve the optimal ascent problem with the indirect method of optimal control are (6)-(12). Solving the problem with the direct method of optimal control only requires the orbital insertion conditions given by equations (6)-(8).

It is important to recognize that the equations shown above are in dimensional form. In numerical optimization, scaling optimization variables appropriately contributes to the efficiency of the algorithm [13]. Variables with similar orders of magnitude result in faster convergence. In this investigation, scaling played an important role in the implementation the ascent problem using the direct method of optimal control, where the algorithm takes longer to converge. Besides longer simulation time, incorrect scaling also caused convergence issues in some cases. One way to accomplish this is by nondimensionalizing the equations required to solve the optimal ascent problem. A common approach is to normalize the distance by the equatorial radius of the planet, velocity by $\sqrt{g_0 R_{eq}}$, and time with $\sqrt{R_{eq}/g_0}$ [14]. The complete set of normalized equations can be found on Ref. [14].

III. Direct and Indirect Methods of Optimal Control

Optimal control problems emerged from a challenge to minimize time in the Brachistochrone problem [15]. Eventually, it expanded to the minimization of more complex problems that require a more formal definition. For an optimal control problem to find a solution, there must exist a state and a control. The control is the element that drives the state by giving it the command to build a trajectory to reach a final state. The last component of an optimal control problem is a cost function or performance index that defines the parameter to be minimized. Nowadays, an optimal control problem is defined as finding the control required to transition a state from an initial condition to a final condition while minimizing the performance index [16]. Additionally, constraints on the trajectory or the endpoints can be added to the problem. Optimal control problems need to be solved numerically due to the difficulty in finding an analytical solution. To solve the problem numerically, it must be implemented as a direct or an indirect method [17]. Each of these methods makes use of the Pontryagin's Minimum Principle, despite having significant differences in formulation. In the direct method of optimal control, the problem is transcribed into a nonlinear programming problem (NLP) by discretization of the state and control functions [18]. The problem is solved using optimization algorithms to find the minimum value of the cost function. The indirect method requires the calculus of variation to find the first-order optimality conditions [19]. The problem is solved as a multi-point boundary value problem (MPBVP). Solving a system of nonlinear equations results in the optimal control solution. The following are two examples of algorithms that implement the direct and indirect methods. These algorithms were employed for the results of this paper.

A. Implementation of the Indirect Method with the Universal Powered Guidance (UPG)

The Universal Powered Guidance (UPG) is a three-dimensional optimal powered guidance formulated on the indirect method of optimal control [10]. It is a multipurpose optimal control algorithm that has been applied to various scenarios such as descent, ascent, deorbit, and orbital transfers [20–22]. The ascent version of the algorithm is labelled UPG+A, but it will simply be referred as UPG for the remainder of this paper.

Based on Pontryagin's Maximum Principle, this method follows the necessary conditions of optimal control. The dynamics and performance index of the problem are as defined by equations (1)-(5). Seven nonlinear algebraic equations on the orbital insertion conditions, transversality conditions and Hamiltonian for a final free-time problem are specified in equations (6)-(12). Given some initial conditions and a final targeting condition, the problem is formulated as a two-point boundary value problem (TPBVP). The 7 nonlinear algebraic equations are solved simultaneously as a root-finding problem in closed-form using the Powell's dogleg optimization method. The optimization method requires an initial guess to solve the problem. The optimal solution finds the control and trajectory that satisfies all seven nonlinear algebraic equations. The thrust direction is found as the optimal solution that minimizes the performance index.

B. Implementation of Direct Method with OpenMDAO

OpenMDAO is a Multidisciplinary Design Optimization (MDO) framework used to solve large-scale optimization problems efficiently [23]. It was initially developed to solve large-scale design problems with coupled numerical models. The need to implement modern algorithms with better efficiency resulted in a new problem structure that improved performance by taking advantage of hierarchical strategies, distributed-memory parallelism, and high-performance computing [23]. Although OpenMDAO was initially developed for large-scale design optimization problems, its efficiency and simplicity facilitate the use in multiple applications [23].

In this study, OpenMDAO was used to verify and validate the results obtained previously with UPG in Ref. [9] and new discoveries developed in this paper. A version of the fuel-optimal ascent problem based on the direct method was implemented in OpenMDAO. The problem was transcribed as an NLP and solved with gradient-based optimization using Newton-type algorithms. Since transversality conditions and the Hamiltonian are not required, only equations (1)-(8) are considered. The system dynamics are defined as ordinary differential equations (ODEs). Time steps are vectorized by a parallel time integration algorithm, while a framework of linear methods is used for numerical integration [24]. In the implementation, an Explicit Midpoint method was utilized to solve the problem without sacrificing too much computational efficiency.

Table 1 Initial Conditions for a Crewed Landing Mission on the South Pole of the Moon [9]

Initial Condition	Value
altitude (km)	15.24
longitude (deg)	41.85
geocentric latitude (deg)	-71.6
inertial velocity (m/s)	1,698.3
inertial topocentric flight path angle (deg)	0.0
inertial topocentric azimuth angle (deg)	180.0
downrange (km)	559.41
crossrange (km)	0.48
total vehicle mass (kg)	15,103
total fuel mass (kg)	10,624
vehicle dry mass (kg)	4,479

IV. Analysis of Solution and Verdict

A. Nominal Powered Descent Abort Mission

The Apollo Lunar Module (LM) was used as the vehicle in the simulations of this study [25]. The LM propulsion system is divided in a descent propulsion system (DPS) and an abort guidance system (AGS) [8]. The descent propulsion system (DPS) is used in both powered descent and abort guidance solutions to emulate a sudden emergency scenario. A total of 45,000 N of thrust are available with the DPS. The specific impulse of the engine is of 311 sec. All the remaining fuel in the vehicle at the time of abort is assumed to be available. The nominal powered descent part of the mission was conducted by the Fractional Polynomial Powered Descent Guidance (FP2DG) for lunar landing mission [26]. The landing location is at the South Pole of the Moon. The initial conditions of the mission are the same as those in Ref. [9] and listed in Table 1. The pull-up maneuver was solved by the Universal Powered Guidance (UPG+A). The fuel-optimal ascent guidance is the only part of the mission that is relevant to the results of this paper. The powered descent and pull-up maneuver are necessary to obtain the initial conditions for the fuel-optimal ascent guidance, but their terminal conditions do not affect the discovery of this investigation. The target orbit for all abort scenarios is a 10 km x 150 km pericynthion orbit around the Moon. The orbit has a 90 deg inclination and a perilune altitude of 10 km. Simulations were performed in 3 degrees-of-freedom (3DOF) with a guidance update rate of 2 Hz and a perfect navigation. UPG + A was used to solve the fuel-optimal ascent guidance.

B. Discovery of Multiple Optima in Fuel-Optimal Ascent Guidance

The novel abort guidance developed in Ref. [9] has shown that a solution to the complex problem of inserting a spacecraft safely into a specified final lunar orbit can be found online. This can be achieved during the entire powered descent trajectory using the indirect method of optimal control. The method utilizes an advanced propellant-optimal guidance algorithm called the Universal Powered Guidance (UPG). In this methodology, the abort guidance problem is implemented as a two-phase maneuver: a pull-up phase and a fuel-optimal ascent guidance. In both abort phases, thrust is kept at its maximum level to ensure a fast transition to the final orbit. In the first phase, the pull-up maneuver is responsible of changing the velocity vector of the vehicle from its current state towards a more favorable direction to begin ascent. It does this by increasing the initial flight path angle from a negative initial value to a positive value. In the second phase, the optimal ascent guidance (UPG+A) takes over starting from the final state of the pull-up maneuver and guides the spacecraft towards a safe pericynthion orbit around the Moon.

A set of "free-attachment" orbital insertion conditions are used to allow maximum flexibility to achieve the specified orbit. The true anomaly at the orbital insertion point is kept free for the guidance to find. This allowed the algorithm to select the optimal final position and velocity regardless of where the actual insertion occurs in the orbit. The advantage of the free-attachment point is that the algorithm is free to choose the best orbital insertion condition in every abort scenario. Within UPG, a system of 7 nonlinear algebraic equations is solved as a root-finding problem to find the thrust direction vector and time-to-go ($t_{go} = t_f - t_0$) to reach the abort orbit [10]. Depending on the selection of the targeting conditions, the 7 algebraic equations are a combination of orbital insertion conditions and their corresponding transversality conditions [12]. The Powell's trust-region method is used to effectively solve the system of equations. Simulations revealed that UPG can achieve the desired orbit from anywhere along the powered descent trajectory wherever it is physically feasible [9].

Despite the successful results obtained by the abort guidance algorithm, an unexpected phenomenon appeared among the solutions without a clear explanation. In each of the abort cases tested, the algorithm reached the orbital insertion conditions successfully. In most cases, the altitude corresponding to the orbital insertion conditions followed a consistent pattern, see Fig. 2 from 0 to 200 seconds and 300 to 600 seconds. However, a cluster of cases between 200 and 250 seconds converged successfully to a lower altitude than the rest of the solutions. See the cluster in Fig. 2 between 200 and 250 seconds. A closer examination of the final conditions confirmed that the spacecraft ended in the correct orbit in these "out-of-family" cases. Figure 3 shows the propellant consumption of every abort case along the powered descent. In all cases, propellant increases as the abort cases start later in the descent.

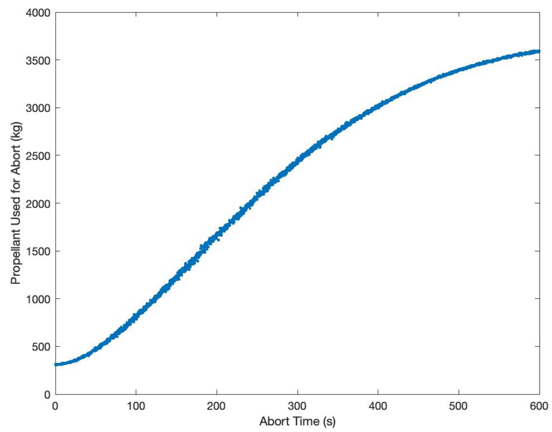

Fig. 3 Propellant Consumed by Abort Cases at Different Points along the Powered Descent Trajectory

The latest abort guidance approach solved the problem of a contingency during descent; however, it left one question unanswered: Why are some of the solutions ending at different altitudes? Looking at the results, it was evident that all trajectories successfully converged to a correct solution. This was confirmed by the agreement found by the fuel consumption comparison among neighboring solutions. In all cases, fuel consumption increased as expected without any jumps or discontinuities. The abort cases converging to a lower altitude followed the system dynamics and ended at a feasible solution. The fact that the algorithm implemented a free attachment point raised some questions about the way in which these points were being chosen by the algorithm. The first encounter of a difference in orbital insertion conditions was found in the true anomaly at the time of orbit insertion. Fig. 4 shows the true anomaly at insertion for each of the abort cases studied.

This figure reveals two curves that encompass all the potential final true anomaly angles for the abort cases in this study. An upper curve for cases that started an abort between 0 and 340 seconds and a lower curve that includes cases for aborts from 340 to 600 seconds. The cases in the higher curve insert the vehicle at a true anomaly angle between 10 and 30 degrees, while the lower curve inserts vehicles at true anomaly angles between -25 and 3 degrees. Unexpectedly, some of the cases that were predicted to fall under the upper curve ended in the lower curve. These cases were the same that formed part of the out-of-family cluster found before!

The plot of true anomaly at insertion point gave an insight into one of the possible reasons to the existence of a discontinuity. To understand the cause of the mismatch, a new approach was developed to investigate this phenomenon. A fixed orbital insertion point was selected instead of the free attachment point used previously. This allowed the exact angle of insertion into the orbit to be chosen by the user. The new strategy consisted in solving the ascent guidance problem at different true anomaly angles on the same final orbit. The final orbit was defined by the known semi-major axis, eccentricity, and inclination. These orbital insertion parameters along with the user-selected true anomaly were used to calculate the final position, velocity, and flight path angle required to insert the spacecraft into the abort orbit. Unlike the free-attachment solution that optimized for the orbit insertion point, in the fixed-point solution it is required to specify the position, velocity, inclination and flight path angle of the desired final condition. Thus, leaving the

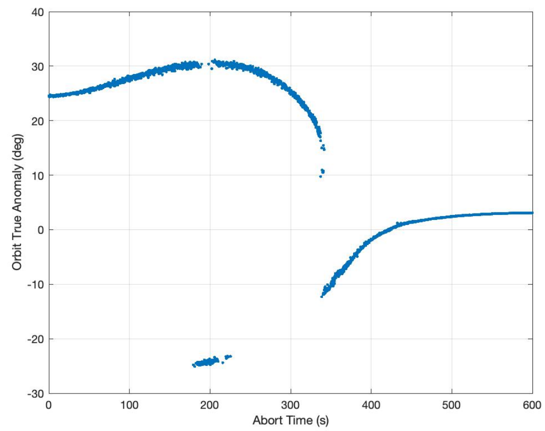

Fig. 4 True Anomaly at Orbital Insertion Point

arguments of periapsis and ascending node as free parameters.

Abort cases activated at every 100 seconds along the powered descent trajectories were selected and their initial conditions recorded. Using the initial conditions for each case, a true anomaly scan between -100 deg to 100 deg was performed to investigate changes in propellant consumption as the spacecraft entered the orbit at different points. Each angle in this range was solved to generate a total of 201 solution points and optimal fuel consumption at each true anomaly angle was recorded. This range was selected to compare the behavior of the algorithm before and after perilune. Cases at different abort times during powered descent were selected for testing. Figure 5 displays the propellant consumption of the spacecraft at different insertion points along the final orbit caused by changes in true anomaly.

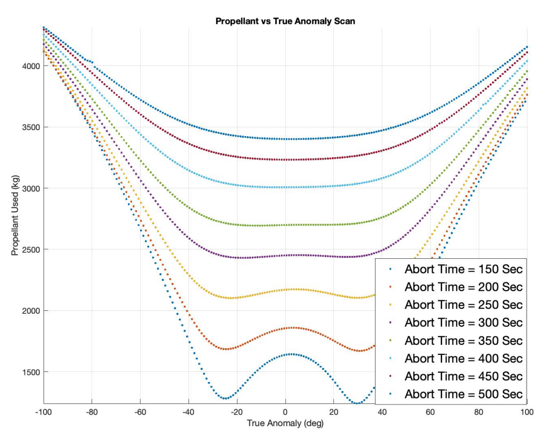

Fig. 5 Propellant Consumption at Different Insertion Points along the Final Orbit

Each curve in Fig. 5 represents the propellant consumption for an abort guidance with the same initial conditions. The different points along the curve represent a different orbital insertion true anomaly. The bottom curve represents an abort case activated at 150 seconds from PDI, while the case at the top represents an abort case activated at 500 seconds from PDI. As we move along the powered descent trajectory, contingencies arise at later times and the optimal solution changes. The true anomaly scan shows the evolution of the propellant curve as abort guidance is initiated at different times. Early on, the curves are more pronounced and characterized by two minima, but they transform into a global minimum as the abort guidance is activated afterwards. The fact that the solution changes from two minima to a single global minimum can be explained by the fact that early on the algorithm has more space and flexibility to decide which way to go. That is, for some time, the flight time from the initial conditions to the two local minima is roughly the same and the difference in propellant consumption is negligible. This surprising result shows that more than one local minimum exists for the same abort cases at different orbital insertion conditions. Figure 6 is a representation of the two guidance solutions available for abort cases early in the descent.

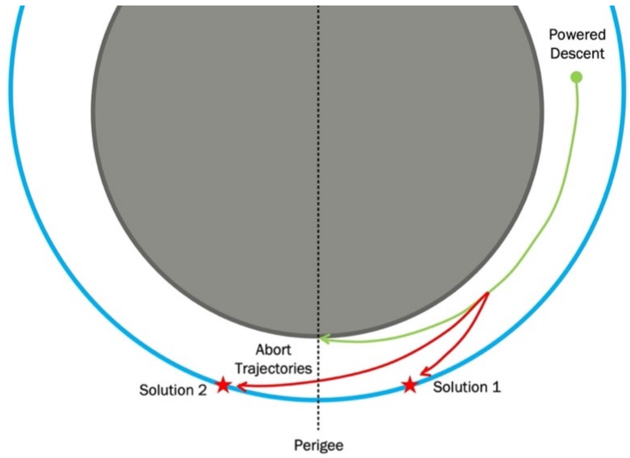

Fig. 6 Representation of Multiple Ascent Solutions in Abort Scenario at the Moon

Notice that both solutions end at the same orbit despite entering at a different true anomaly angle. In each curve, one of the solutions is a local minimum and the other is a global minimum. The global minimum appears to favor a positive true anomaly after perilune. Further analysis showed that the global minima is always associated with the solution at the highest altitude, but that the propellant consumption differs by a very small amount. The fact that in some cases the solution ends at a different altitude means that the algorithm found the local solution instead of the global solution. It is evident that the previously unanswered phenomenon is a result of this property. The altitude pattern that most abort trajectories follow corresponds to the global minimum from the propellant consumption curve. However, there are some cases that end up trapped in the sphere of influence of the other local minimum that has a similar propellant consumption.

Furthermore, as the descent progresses, aborting from a lower altitude becomes more challenging and the algorithm starts to lose some leeway. Eventually, there is only one clear optimal solution, and the algorithm must choose that orbital insertion point. The orbit perilune, defined as 10 km for this problem, is the closest point from the orbit to the Moon. The latest cases start abort at an altitude below perilune, therefore the only possible solution is to abort to perilune. Only abort cases that begin after 400 seconds are guaranteed to find a unique global minimum. These cases begin ascent at an altitude below perilune, and the only possible solution is to target perilune. It should be recognized that perilune is not fixed to a specific point relative to the Moon and can be changed by the guidance solution. Given that abort is such an important safeguard of a landing mission, exploring the solution and getting answers to all the unknown behavior is the focus of this work. The implications of this discovery are important to understand any potential drawbacks or unexpected situations that might arise from abort maneuvers. In addition, future missions to the Moon can take advantage of this discovery for mission planning or astronaut training. Since the possibility to abort into the same orbit at a different altitude is present for a big part of the descent, it is important to be aware that such a situation might emerge. Should there be any question about the expected ending conditions during a particular mission to the Moon, the information revealed here has the potential to influence the selection of the best decision given a particular scenario.

V. Validation and Verification

Validation and verification (V&V) of the algorithm was performed to establish confidence in the results. The solution to the abort guidance problem was obtained by UPG, an optimal control guidance algorithm based on the indirect method of optimal control. Considering that a spacecraft landing on the Moon would require onboard computation to perform all the maneuvers, the indirect method finds a fast and reliable solution to the abort problem. However, replicating these results with a different method would confirm the accuracy and validity of the solution.

To corroborate these results, we resorted to the direct method of optimal control in which the problem is solved as a nonlinear programming problem. The goal is to provide a comparison with a clear agreement between the direct and indirect method solutions. For the direct method approach, the abort guidance problem was solved using an open-source

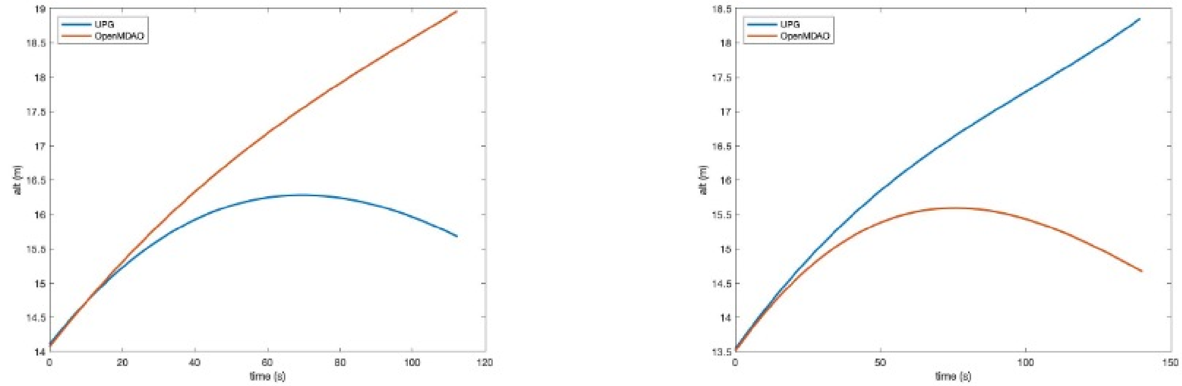

(a) (b)

Fig. 7 (a) Optimal ascent trajectory when abort is activated at 200 seconds after PDI (b) Optimal ascent trajectory when abort is activated at 250 seconds after PDI

software named OpenMDAO. Solving with both methods would allow us to trust that the algorithm is finding the correct solution. Since both methods solve the problem differently, matching the solutions would signify that we can trust both algorithms with great confidence.

In testing, the free-attachment problem was implemented to allow the algorithm to optimize the orbital insertion condition. The formulation with the direct method consisted in implementing the equations (1)-(8) in the abort guidance problem. The transversality conditions and the Hamiltonian are not required to solve the problem with the direct method of optimal control. OpenMDAO was able to successfully obtain a solution to all the abort scenarios analyzed, thus giving confidence that the formulation with both methods was appropriate and that the solution is trustworthy. Furthermore, it was shown that most abort scenarios converged to the same solution and followed the same trajectory in both methods. The outcomes of the analysis demonstrated the effectiveness of UPG to find an optimal solution. Notwithstanding, an unexpected revelation showed that some of the abort scenarios analyzed with OpenMDAO converged successfully to different final conditions than those from UPG. This was surprising since this behavior was only evident in selected abort cases solved with UPG. In Fig. 2, this outcome is shown for two cases that initiated abort at 200 and 250 seconds after PDI.

In Fig. 7a, the solution with UPG inserts the vehicle at an altitude of 19 km, while the solution with OpenMDAO does the same but ends at an altitude of close to 15.5 km. The difference between both solutions is of more than 3 km. Similarly, in Fig. 7b, the solution obtained by UPG enters orbit at close to 18.4km, while OpenMDAO ends at 14.6 km. In this case, the difference is of almost 4 km. Note that in both cases, even though the solution ends at different altitudes, the total flight time is essentially the same. Since thrust is always at full throttle, this means that the propellant consumption is indistinguishable in both trajectories. The reason this result is surprising is because the solution that gives the highest altitude in both cases alternates between UPG and OpenMDAO. Before this comparison, the multiple optima were noticed in the solution with UPG. Since each one of these methods converged to a viable solution, detecting multiple solutions with the direct and indirect methods implies that this behavior is not dependent on the implementation, or the method used. Effectively, any method that finds an optimal solution to the abort guidance problem will encounter this phenomenon. This reiterates the belief that this discovery is an important tool for contingency planning in preparation for future missions to the Moon.

Motivated by this new discovery and certain that the results found with the indirect method could be replicated with the direct method. A new true anomaly scan was performed using the direct method of optimal control to examine the propellant consumption obtained with this method. The propellant curve for varying true anomalies is presented in Fig. 8.

The resulting propellant consumption at different orbital insertion points exhibited the same behavior with OpenMDAO. Albeit more computationally expensive, a closer look revealed that the propellant curve matched exactly the curves obtained with UPG. The existence of multiple optima is evident in both cases and confirms the results obtained previously. In Fig. 9, a glance at the abort solutions for cases throughout the descent exposes their ascent

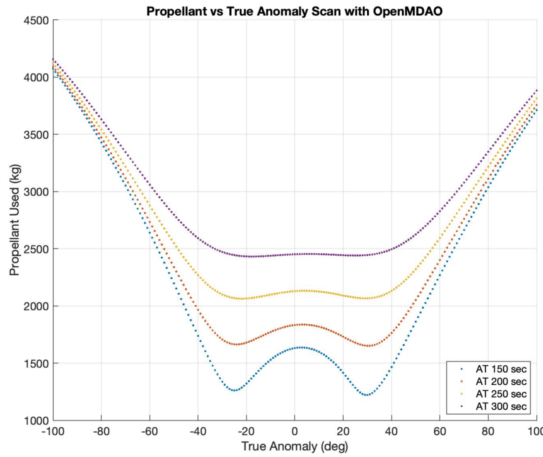

Fig. 8 Propellant vs True Anomaly Scan with OpenMDAO

trajectories.

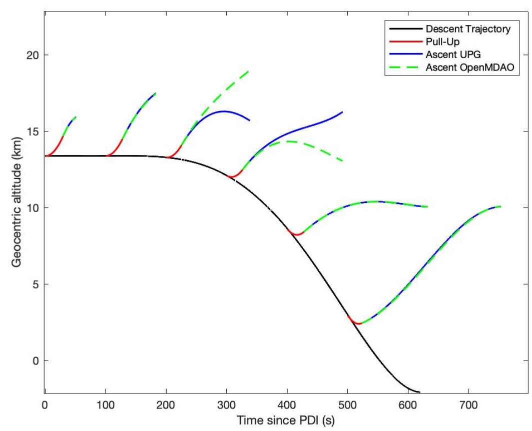

Fig. 9 Abort Solutions at different points along the powered descent trajectory

Starting from a powered descent trajectory generated by FP2DG, abort can begin at any time during the descent. The complete abort solution presented in Ref. [9] performs a pull-up maneuver to align the vehicle and a fuel-optimal ascent guidance to determine the best orbital insertion condition. The black line represents the powered descent guidance without any abort and the red portion is the pull-up maneuver. The fuel-optimal ascent guidance is differentiated by a continuous blue line for UPG and a dashed green line for OpenMDAO. In this paper, only the fuel-optimal ascent guidance is involved in the multiple optimal solution.

Abort cases initiated at the first or final portion of the descent converge to the same solution. At the beginning, the initial conditions and initial guess of the optimization algorithm favor the global minimum. Although the propellant curve reveals a more pronounced minima for earlier cases, it seems that the position of the vehicle and the direction of the ascent trajectory benefit an insertion into the orbit before perilune. On the other hand, cases closer to the end of the descent are bound to only one solution at perilune. The middle portion of the trajectory contains all the cases that exemplify the subject of having multiple solutions to the same problem. Cases in the middle are more complex, as they depend on the initial conditions of the problem, the initial guess and the type of optimization method used. Using the final ascent conditions, the true anomaly at insertion can be calculated for each case. Figure 10 combines the true anomaly calculated with the propellant curve for 3 different abort cases and unveils important information about the orbital insertion altitude as a function of true anomaly.

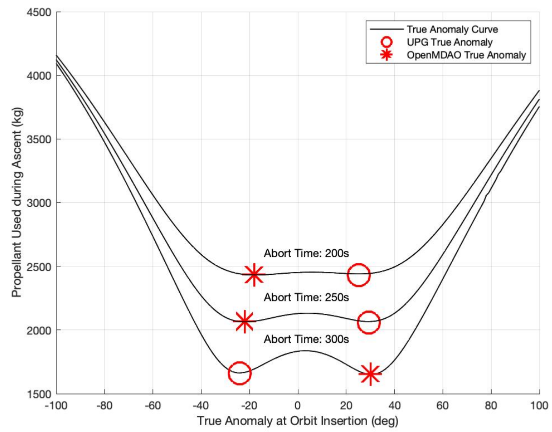

Fig. 10 True anomaly at insertion point

Propellant curves for abort cases starting at 200, 250 and 300 seconds are plotted. These cases were selected because they are part of the cluster cases for both UPG and OpenMDAO. Each of these cases clearly shows the two local minima. Adding the true anomaly resulting from the orbital insertion conditions for these cases demonstrates that the difference in altitude is related to the true anomaly at insertion point, with a higher altitude entering at a negative true anomaly, while the lower altitude enters orbit at a positive true anomaly. The uncovering of multiple solutions gives reassurance on the nature of this phenomenon. Every abort scenario has at most two solutions and neither of them are arbitrary. Understanding the solution helps predict the outcome of an emergency before it happens. Furthermore, knowing that both solutions are near fuel-optimal allows the manipulation of the solution to be forced to enter the orbit at a specific location.

The last component of this investigation involved a more detailed inspection on the nature of the cluster cases in the middle. A comparison of the results obtained by OpenMDAO and UPG would give an insight on the similarities and differences among these cases. A comparison of the ascent trajectories for some abort cases between 200 and 300 seconds after PDI is shown in Fig. 11.

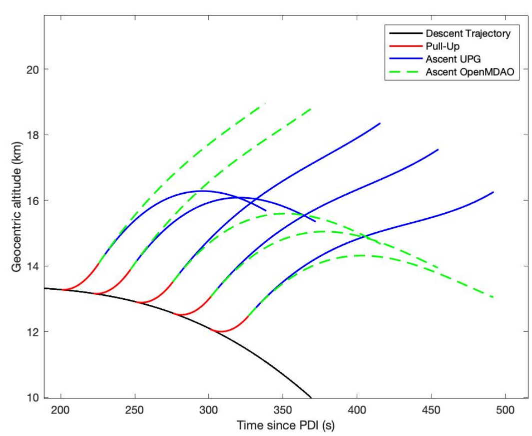

Fig. 11 Abort Trajectories in cluster converging to different altitude

In the case of OpenMDAO, it appears that the cluster of cases ending at a lower altitude starts a little bit later. The ascent solution by UPG converges to a lower solution in cases that started abort at 200 and 225 seconds, while OpenMDAO converges a higher altitude in the same cases. On cases that started abort at 250, 275 and 300 seconds, OpenMDAO converges to a lower altitude, while UPG enters orbit at a higher altitude. Due to the computational time expense of the direct method, 3000 Monte Carlo simulations were not performed with this method. But a small experiment with UPG revealed that changing the initial guess of the optimization method influences the range of the cluster cases. For instance, the nominal ascent guess time for UPG is of 200 seconds. Reducing the ascent guess time caused the cluster cases to shift to the left, while increasing the guess time caused them to move to the right. Changing the initial guess time did not eliminate the cluster. Although OpenMDAO utilizes a vector of normalized times rather than an initial guess, it is possible that the mechanism used to solve the solution acts similar than the initial guess implemented in UPG. This would explain the different ranges found for each method. This is merely an observation that goes beyond the scope of this paper.

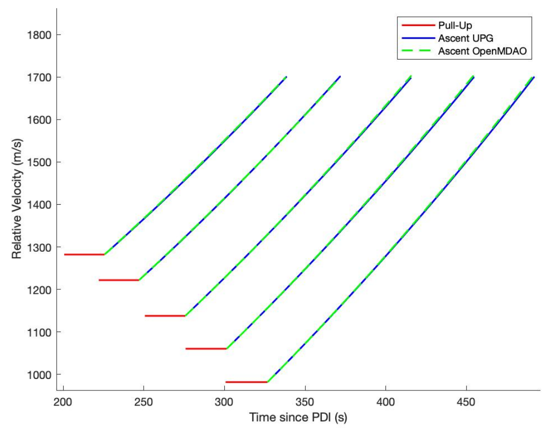

Fig. 12 Velocity profiles for different abort cases in the cluster

Additionally, velocity profiles for each abort case revealed similar patterns among all solutions. Figure 12 shows a velocity profile comparison for the cluster cases tested. This demonstrated that the velocity is the same using both methods, regardless of the final altitude achieved. The implication of this result means that the propellant consumption should be very close among solution to the same case using different methods. The fact that the velocity profiles were identical, implied that the total ascent time must be similar since both implementations are running at full throttle. This was confirmed by the propellant comparison in Fig. 13.

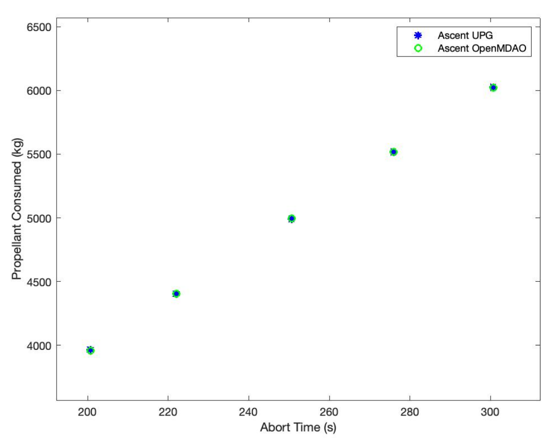

Fig. 13 Propellant Consumption Comparison between Direct and Indirect Solutions

Propellant consumption increases as the abort occurs later in the descent. Since the vehicle gets closer to the ground as it moves through the descent trajectory, it requires more propellant to ascend into the final orbit. The propellant consumption among the cluster cases tested is indistinguishable between the two methods. This means that both solutions are near-optimal despite entering the final orbit at a different altitude. Knowing that either solution is near-optimal, there is no impact in propellant efficiency by the selection of a specific final altitude. The discovery of the two minima in the propellant curve indicates that at every point before 400 seconds, multiple fuel-optimal ascent solutions exist. This is an important discovery for crewed lunar landing missions on the grounds that in case of a contingency, the crew and support team should be prepared to encounter this type of behavior. The only concern is to be able to predict the altitude that the algorithm will choose at any given time. This could be predicted by testing different initial conditions in Monte Carlo simulations.

Although a spacecraft insertion to a lower altitude is also a safe solution to the abort ascent problem, it is not ideal to deviate from the rest of the solutions. This is especially concerning if the propellant consumption is the same and there is no added benefit to take a different route. Furthermore, being unaware of the expected result is an idea that goes opposite to the principle of contingency. Perhaps a better solution is to require the guidance to end above a specific altitude in case of abort. This can be accomplished by forcing the solution to insert the vehicle at a negative true anomaly. Multiple methods can be implemented to ensure that the guidance selects a particular solution. The important takeaway is that lnowledge of the two possible solutions enables multiple approaches to influence the result. The fact that the final condition can now be predicted is the greatest advantage of this discovery.

VI. Conclusion

In any human mission, the priority is the safety of the crew. A great deal of attention is spent on the guidance, navigation and control system to create redundancy and reduce the risks involved in space missions. One such component of GNC is the abort capability that the spacecraft possess to take a spacecraft from an emergency situation into a secure orbit around the Moon. The problem of abort guidance during lunar powered descent was finally resolved with an innovative approach that updated abort guidance methods that were in place since the Apollo missions. Among the set of solutions obtained from this new algorithm, an unexpected phenomenon caused some of the abort trajectories to converge to a different altitude than anticipated. In this paper, an analysis of the abort solution finally puts an end to the unsolved mystery. A new fixed-point formulation allowed the discovery of multiple optima on many of the abort guidance solutions. This realization gives a better understanding of the characteristics of an abort trajectory and allows future missions to plan in advance for this phenomenon. The results found in this study are not unique to this implementation and will emerge in similar optimal control approaches. The implications of this finding pertain the contingency planning in future missions to the Moon. Validation and verification of the algorithm is performed to demonstrate the efficacy of the algorithm and the reliability of the solution.

Acknowledgments

The authors would like to thank the NASA Space Technology Research Fellowship Grant Number 80NSSC18K1170 for the support to develop this project.

References

[1] Emme, E. M., "Historical persepectives on Apollo," *Journal of Spacecraft and Rockets*, Vol. 5, No. 4, 1968, pp. 369–382. https://doi.org/10.2514/3.29263.

[2] Nassiff, S. H., and Martikan, F. O., "Integrated operating mode of the Apollo mission simulator," *Journal of Spacecraft and Rockets*, Vol. 2, No. 6, 1965, pp. 1005–1007. https://doi.org/10.2514/3.28344.

[3] Cheatham, D. C., and Hackler, C. T., "Handling qualities for pilot control of Apollo lunar-landing spacecraft." *Journal of Spacecraft and Rockets*, Vol. 3, 1966, pp. 632–638. https://doi.org/10.2514/3.28506.

[4] Lindquist, O. H., "Development of a manual thrust-vector-control mode for Apollo," *Journal of Spacecraft and Rockets*, Vol. 5, No. 3, 1968, pp. 297–302. https://doi.org/10.2514/3.29242.

[5] Siller, J. F., "SYNOPTIC: Full-scale Apollo Docking Simulation Tests," *Journal of Spacecraft and Rockets*, Vol. 7, No. 8, 1970, pp. 956–957. https://doi.org/10.2514/3.59644.

[6] Martin, F. H., and Battin, R. H., "Computer-controlled steering of the Apollo spacecraft," *Journal of Spacecraft and Rocekts*, Vol. 5, No. 4, 1968, pp. 400–407. https://doi.org/10.2514/3.29267.

[7] Hyle, C. T., E.Foggatt, C., and Weber, B. D., "Apollo Experience Report - Abort Planning," Technical Note D-6847, NASA, 1972.

[8] Kurten, P. M., “Apollo Experience Report-Guidance and Control Systems: Lunar Module Abort System,” Technical Note D-7990, NASA, 1975.

[9] Lu, P., and Sandoval, S. A., “Abort Guidance during Powered Descent for Crewed Lunar Missions,” *AIAA SciTech 2021 Forum and Exposition*, AIAA Paper 2021-0505, 2021. https://doi.org/10.2514/6.2021-0505.

[10] Lu, P., “Propellant-Optimal Powered Descent Guidance,” *Journal of Guidance, Control, and Dynamics*, Vol. 41, No. 4, 2018, pp. 813–826. https://doi.org/10.2514/1.G003243.

[11] Jezewski, D. J., “An optimal, analytic solution to the linear- gravity, constant-thrust trajectory problem,” *Journal of Spacecraft and Rockets*, Vol. 8, No. 7, 1971, pp. 793–796. https://doi.org/10.2514/3.30320.

[12] Pan, B., Chen, Z., Lu, P., and Gao, B., “Reduced Transversality Conditions in Optimal Space Trajectories,” *Journal of Guidance, Control, and Dynamics*, Vol. 36, No. 5, 2013, pp. 1289–1300. https://doi.org/10.2514/1.60181.

[13] Ross, I. M., Gong, Q., Karpenko, M., and Proulx, R. J., “Scaling and Balancing for High-Performance Computation of Optimal Controls,” *Journal of Guidance, Control, and Dynamics*, Vol. 41, No. 10, 2018, pp. 2086–2097. https://doi.org/10.2514/1.G003382.

[14] Lu, P., Griffin, B. J., Dukeman, G. A., and Chavez, F. R., “Rapid Optimal Multiburn Ascent Planning and Guidance,” *Journal of Guidance, Control, and Dynamics*, Vol. 31, No. 6, 2008, pp. 1656–1664. https://doi.org/10.2514/1.36084.

[15] Ross, I. M., *A Primer on Pontryagin’s Principle in Optimal Control*, 2$^{\text{nd}}$ ed., Collegiate Publishers, San Francisco, 2015, Chaps. 1-2, pp. 1–170.

[16] Kirk, D. E., *Optimal Control Theory: An Introduction*, Dover Publications, Inc., Mineola, New York, 2004.

[17] Negarchi, N., and Nouri, K., “A New Direct Method for Solving Optimal Control Problem of Nonlinear Volterra-Fredholm Integral Equation via the Müntz-Legendre Polynomials,” *Bulletin of the Iranian Mathematical Society*, Vol. 45, No. 3, 2019, pp. 917–934. https://doi.org/10.1007/s41980-018-0173-z.

[18] Böhme, T. J., and Frank, B., *Hybrid Systems, Optimal Control and Hybrid Vehicles: Theory, Methods and Applications*, Springer International Publishing, Cham, 2017, Chap. 8, pp. 233–273. https://doi.org/10.1007/978-3-319-51317-1_8.

[19] Rao, A. V., “A Survey of Numerical Methods for Optimal Control,” *AAS/AIAA Astrodynamics Specialist Conference*, AAS Paper 09-334, Pittsburgh, PA, 2009.

[20] Lu, P., and Pan, B., “Highly Constrained Optimal Launch Ascent Guidance,” *Journal of Guidance, Control, and Dynamics*, Vol. 33, No. 2, 2010, pp. 404–414. https://doi.org/10.2514/1.45632.

[21] Baldwin, M., and Lu, P., “Optimal Deorbit Guidance,” *Journal of Guidance, Control, and Dynamics*, Vol. 35, No. 1, 2012, pp. 93–103. https://doi.org/10.2514/1.53937.

[22] Lu, P., Forbes, S., and Baldwin, M., “A Versatile Powered Guidance Algorithm,” *AIAA Guidance, Navigation, and Control Conference*, AIAA Paper 2012-4843, Minneapolis, MN, 2012. https://doi.org/10.2514/6.2012-4843.

[23] Gray, J. S., Hwang, J. T., Martins, J. R. R. A., Moore, K. T., and Naylor, B. A., “OpenMDAO: an open-source framework for multidisciplinary design, analysis, and optimization,” *Structural and Multidisciplinary Optimization*, Vol. 59, No. 4, 2019, pp. 1075–1104. https://doi.org/10.1007/s00158-019-02211-z.

[24] Hwang, J. T., and Munster, D., “Solution of ordinary differential equations in gradient-based multidisciplinary design optimization,” *2018 AIAA/ASCE/AHS/ASC Structures, Structural Dynamics, and Materials Conference*, AIAA Paper 2018-1646, Kissimmee, FL, 2018. https://doi.org/10.2514/6.2018-1646.

[25] “Apollo 11 Lunar Module / EASEP,” NSSDCA/COSPAR ID 1969-059C, NASA, 1969.

[26] Sandoval, S. A., and Lu, P., “Powered Descent Guidance for a Crewed Lunar Landing Mission,” *2020 AAS Guidance, Navigation, and Control Conference*, AAS Paper 20-044, Breckenridge, CO, 2020.